

Analysis of Modified Franz-Keldysh Effect under Influence of Electronic Intraband Relaxation Phenomena

メタデータ	言語: eng 出版者: 公開日: 2020-05-29 キーワード (Ja): キーワード (En): 作成者: メールアドレス: 所属:
URL	https://doi.org/10.24517/00058216

This work is licensed under a Creative Commons Attribution-NonCommercial-ShareAlike 3.0 International License.



Analysis of Modified Franz-Keldysh Effect under Influence of Electronic Intraband Relaxation Phenomena

Yuji KUWAMURA and Minoru YAMADA

*Department of Electrical and Computer Engineering,
Faculty of Engineering, Kanazawa University,
2-40-20 Kodatsuno, Kanazawa, Ishikawa 920, Japan*

(Received)

Characteristics of the Franz-Keldysh effect were theoretically analyzed by taking into account electronic intraband relaxation. Theoretical analysis of optical absorption was performed basing on the density matrix formalism with the help of a stochastic model to include the intraband relaxation. The absorption tails observed in experiments were well explained by this theoretical analysis, together with the Franz-Keldysh effect itself.

KEYWORDS: density matrix, electronic intraband relaxation, Franz-Keldysh effect, semiconductor optical modulator, electrooptical effect

1. Introduction

The optical absorption coefficient or the refractive index can be controlled with an applied electric field in various materials. Such an electrooptical effect in a bulk semiconductor crystal is called the Franz-Keldysh effect and is utilized as an operation mechanism in optical modulators or switches, which are fundamental devices in optoelectronics.¹⁻⁹⁾ However, the results of theoretical analyses of the Franz-Keldysh effect have not exactly coincided with the experimental data,¹⁰⁻²²⁾ and several modifications are required in order to explain experimental data.⁸⁾ The most noteworthy differences between the theoretical results and experimental data concern the absorption tail²³⁾ which is always observed in an absorption spectrum at photon energies smaller than the band-gap energy even there is no external applied field. The electron transition through the impurity-band formed by impurity atoms was given as an explanation for the absorption tail.

Similar characteristics of the absorption tail in the gain and the spontaneous emission spectrum for photon energies lower than the band-gap energy were also observed in the study of semiconductor lasers. Kane²⁴⁾ theoretically explained that distributing fluctuations of the potential, which is formed by the ionized impurity atoms, create a tail-like density of states in a Gaussian shape. Furthermore, Halperin and Lax²⁵⁾ and Lasher and Stern²⁶⁾ improved this absorption-tail model in a quantum mechanical manner. However, these theoretical analyses treated materials highly doped with impurity atoms, and did not explain why the tail of the gain or the absorption spectrum is still observed in undoped semiconductor crystals.

Yamada and co-workers explained that the tail phenomena are caused by the relaxation effect of the electron wave due to scattering among electrons.^{28,29)} Yamanishi³⁰⁾ and Yamanishi and Lee³¹⁾ also investigated, in more detail, mechanisms of electronic scattering and pointed out that line shape typical of broadening of the spectrum show characteristics intermediate between those of Lorentzian and Gaussian functions. Since the absorption tail was also observed in the quantum well semiconductor

lasers, which are being rapidly developed in recent years with precise fabrication technologies, the electronic intraband relaxation effect has been widely accepted as the origin of the tail on the basis of several detailed theories.³¹⁻³⁴⁾

The most popularly used theoretical method to introduce the electronic intraband relaxation effect is the density matrix formalism in semiconductor lasers.²⁸⁾ In this work, we theoretically analyze the optical absorption basing on the density matrix formalism, but further improve the treatment to determine a more accurate profile of the tail. In the next section, derivation of the dynamic equation of the density matrix element is reexamined using a stochastic model which includes the effect of non-Markovian intraband relaxation. Then a basic equation on optical absorption under the influence of electronic intraband relaxation is derived. In § 3, a form of the optical absorption coefficient under application of external DC electric field is derived by considering the Franz-Keldysh effect together with the relaxation effect. In § 4, numerically calculated examples of the absorption coefficient in GaAs are given. We take into account the electronic transition from the valence band to the conduction band but, for simplicity, do not take into account other transition mechanics such as that through the exciton state or that by free carrier absorption.

2. Method of Density Matrix

2.1 *Damping on dipole vibration with electronic relaxation effect*

It is convenient to use the method of the density matrix for describing the dynamical behavior of a dipole in a semiconductor.³⁵⁾ The time response of the dipole to a continuous optical field is determined with a conventional density matrix $\rho(t)$ or with a matrix element $\rho_{vc}(t)$ given in eqs.(20) and (24). The relaxation effect of the dipole or the electron wave is caused by mutual interaction among the dipoles or the electrons. Then we start here by introducing a subset $w(t)$ of the density matrix to represent, in more details, microscopic characteristics of the dipoles or the electrons. We indicate the principal Hamiltonian corresponding to the band structure in a semiconductor crystal as H_0 , the eigenenergy level of which is W_n at the eigenstate

of $|n\rangle$. We also assume that a time-dependent perturbation $H_r^{(i)}(t)$ is applied to the subsystem of electrons from $t = t_i$. The dynamical behavior of the subset $w(t)$ of the density matrix is given by the following equation:

$$\frac{dw(t)}{dt} = \frac{1}{j\hbar} [(H_0 + H_r(t)) , w(t)]. \quad (1)$$

Equation (1) is transformed into an interaction picture as

$$\frac{dw'(t)}{dt} = \frac{1}{j\hbar} [H_r'(t) , w'(t)], \quad (2)$$

where ' represents "in the interaction picture" in the relations of

$$w'(t) = \exp \left[\frac{H_0 t}{j\hbar} \right] w(t) \exp \left[-\frac{H_0 t}{j\hbar} \right] \quad (3)$$

and

$$H_r'(t) = \exp \left[\frac{H_0 t}{j\hbar} \right] H_r(t) \exp \left[-\frac{H_0 t}{j\hbar} \right]. \quad (4)$$

We solve an approximate solution of eq.(2) using the interaction technique up to the second-order perturbation. When time increases as $t \rightarrow t + \Delta t$, the variation of $w'(t)$ is obtained by

$$\begin{aligned} & w'(t + \Delta t) - w'(t) \\ &= \frac{1}{j\hbar} \int_t^{t+\Delta t} [H_r'(u_1) , w'(t)] du_1 \\ & - \frac{1}{\hbar^2} \int_t^{t+\Delta t} \int_t^{u_2} [H_r'(u_2) , [H_r'(u_1) , w'(t)]] du_1 du_2. \end{aligned} \quad (5)$$

Setting eigenstates in the conduction and valence bands to be $|c\rangle$ and $|v\rangle$, respectively, and writing the off-diagonal element of $w'(t)$ as $w'_{vc}(t)$, the dynamical behavior of a dipole in a semiconductor is determined by the off-diagonal element $w'_{vc}(t)$. By multiplying eq.(5) by $\langle v|$ from the left side and by $|c\rangle$ from the right side, we obtain

the matrix element of $w'(t)$ as

$$\begin{aligned}
& w'_{vc}(t + \Delta t) - w'_{vc}(t) \\
&= \frac{1}{j\hbar} \int_t^{t+\Delta t} f_1(u_1) w'_{vc}(t) du_1 \\
&\quad - \frac{1}{\hbar^2} \int_t^{t+\Delta t} \int_t^{u_2} f_2(u_1, u_2) w'_{vc}(t) du_1 du_2,
\end{aligned} \tag{6}$$

where $f_1(u_1)$ is the term of the first-order perturbation,

$$f_1(u_1) = \langle v | H'_r(u_1) | v \rangle - \langle c | H'_r(u_1) | c \rangle, \tag{7}$$

and $f_2(u_1, u_2)$ is the second-order perturbation,

$$\begin{aligned}
& f_2(u_1, u_2) \\
&= \{ \langle v | H'_r(u_2) H'_r(u_1) | v \rangle + \langle c | H'_r(u_2) H'_r(u_1) | c \rangle \} \\
&\quad - \{ \langle v | H'_r(u_2) | v \rangle \langle c | H'_r(u_1) | c \rangle \\
&\quad\quad + \langle v | H'_r(u_1) | v \rangle \langle c | H'_r(u_2) | c \rangle \}.
\end{aligned} \tag{8}$$

It is known that contributions of the third and fourth terms in eq.(8) are eventually negligible in a semiconductor crystal.^{30, 36)}

We take here the statistical average of eq.(6) over the system, as indicated by $\overline{\quad}$. Since the statistical average of the perturbation $H'_r(t)$ is $\overline{\langle n | H'_r | n \rangle} = 0$, the term with the first-order perturbation in eq.(6) must become zero.

The variables u_1 and u_2 in the second-order perturbation in eq.(6) vary in the range of $t \leq u_1 \leq u_2 \leq t + \Delta t$ for a short time interval Δt . However, the statistical average must be performed over $t_i \leq t \leq u_2$, because the interaction starts from $t = t_i$. Then, we rewrite

$$\overline{f_2(u_1, u_2)} = \int_{t_i}^{u_2} \overline{f_2(t, u_2)} \delta(t - u_1) dt. \tag{9}$$

The time interval $u_2 - t_i$ is long enough to define the autocorrelation of $H'_r(t)$. we assume here that the fluctuated Hamiltonian is characterized by the second-order

correlation in a semiconductor crystal³⁶⁻³⁸⁾ as

$$\frac{1}{\hbar^2} \overline{f_2(t, u_2)} = A \exp\left(-\frac{u_2 - t}{\tau_b}\right), \quad (10)$$

where A is the amplitude of the fluctuation and τ_b is the correlation time of the fluctuation. Therefore, we can write

$$\begin{aligned} & \frac{1}{\hbar^2} \int_t^{t+\Delta t} \int_t^{u_2} \overline{f_2(u_1, u_2)} du_1 du_2 \\ &= \frac{1}{\hbar^2} \int_t^{t+\Delta t} \int_{t_i}^{u_2} \overline{f_2(s, u_2)} ds du_2 \\ &= \Delta t \int_0^{t-t_i} A \exp\left(-\frac{\tau}{\tau_b}\right) d\tau. \end{aligned} \quad (11)$$

Then the statistical average of eq.(6) becomes

$$\begin{aligned} & \overline{w'_{vc}(t + \Delta t)} - \overline{w'_{vc}(t)} \\ &= -\Delta t \int_0^{t-t_i} A \exp\left(-\frac{\tau}{\tau_b}\right) d\tau \overline{w'_{vc}(t)}, \end{aligned} \quad (12)$$

which is rewritten in the form of a dynamic equation as

$$\frac{d\overline{w'_{vc}(t)}}{dt} = -\gamma(t, t_i) \overline{w'_{vc}(t)} \quad (13)$$

with

$$\begin{aligned} \gamma(t, t_i) &= \int_0^{t-t_i} A \exp\left(-\frac{\tau}{\tau_b}\right) d\tau \\ &= \frac{1}{\tau_a} \left\{ 1 - \exp\left(-\frac{t-t_i}{\tau_b}\right) \right\} \end{aligned} \quad (14)$$

and

$$\frac{1}{\tau_a} = A\tau_b. \quad (15)$$

Parameter τ_a may correspond to the intraband relaxation time τ_{in} in the previous density matrix theory.^{28,29)} Substituting eq.(14) into eq.(13), we obtain the solution

for the density matrix element as

$$\overline{w'_{vc}(t)} = \overline{w'_{vc}(t_i)} \exp \left\{ -\frac{\tau_b}{\tau_a} \left(\frac{t-t_i}{\tau_b} + e^{\frac{t-t_i}{\tau_b}} - 1 \right) \right\}. \quad (16)$$

2.2 Response of the density matrix to continuous optical field

Since the rate of relaxation for electronic scattering varies with time t , as discussed in the previous section, it is difficult to give a dynamic equation of the density matrix to represent the response to a continuous optical field. We examine the time response of the density matrix $\overline{w'_{vc}(t)}$ for an impulse $\delta(t - t_i)$ field, in the first step. Then the response to the continuous optical field is examined in terms of $\rho_{vc}(t)$, which corresponds to a matrix element in the conventional density matrix formalism.

When an impulse of the electric field $\delta(t - t_i)$ is applied at the initial time $t = t_i$, variation of $\overline{w_{vc}(t, t_i)}$ in the Schrödinger picture is given as

$$\begin{aligned} \frac{d\overline{w_{vc}(t, t_i)}}{dt} = & -\frac{1}{j\hbar} (\overline{w_{cc}} - \overline{w_{vv}}) R_{vc} \delta(t - t_i) \\ & + \left\{ j\omega_{cv} - \gamma(t, t_i) - \frac{1}{\tau_s} \right\} \overline{w_{vc}(t, t_i)}, \end{aligned} \quad (17)$$

where $\overline{w_{cc}}$ and $\overline{w_{vv}}$ are diagonal elements of the density matrix, R_{vc} is a matrix element of the dipole moment operator, and $\omega_{cv} = (W_c - W_v)/\hbar$ indicates an angular frequency corresponding to the difference between energy levels W_c and W_v in the conduction and valence bands, respectively. The first term in eq.(17) expresses an interaction between the electromagnetic field and the dipole. Terms in the braces mean the resonance effect with ω_{cv} , the electronic relaxation effect characterized by γ , and spontaneous emission with $1/\tau_s$. Since we assumed that the matrix element $\overline{w_{vc}(t, t_i)}$ in eq.(17) starts from the time $t = t_i$, the solution $\overline{w_{vc}(t, t_i)}$ in eq.(17) is obtained by

$$\overline{w_{vc}(t, t_i)}$$

$$\begin{aligned}
&= -\frac{1}{j\hbar}(\overline{w_{cc}} - \overline{w_{vv}})R_{vc} \\
&\quad \times \exp \left\{ j\omega_{cv}(t - t_i) - \int_{t_i}^t \gamma(u_1, t_i) du_1 - \frac{(t - t_i)}{\tau_s} \right\}.
\end{aligned} \tag{18}$$

The continuous optical field is expressed by setting the complex amplitude E_ω and the angular frequency ω of the electric field as

$$E(t) = E_\omega e^{j\omega t} + E_\omega^* e^{-j\omega t}. \tag{19}$$

Writing the response of the density matrix to the continuous optical field as $\rho_{vc}(t)$, $\rho_{vc}(t)$ is given by the superposition of $\overline{w_{vc}(t, t_i)}$ which starts from various initial times t_i . Therefore,

$$\begin{aligned}
\rho_{vc}(t) &= \int_{-\infty}^t \overline{w_{vc}(t, t_i)} (E_\omega e^{j\omega t_i} + E_\omega^* e^{-j\omega t_i}) dt_i \\
&\approx -\frac{1}{j\hbar} (\rho_{cc} - \rho_{vv}) R_{vc} \Phi(\omega) E_\omega e^{j\omega t},
\end{aligned} \tag{20}$$

where $\Phi(\omega)$ gives a spectral line shape,

$$\Phi(\omega) = \int_0^\infty \exp\{j(\omega_{cv} - \omega)\tau - \Gamma(\tau)\} d\tau, \tag{21}$$

and the coefficient $\Gamma(\tau)$ is defined as

$$\Gamma(\tau) = \int_{t-\tau}^t \gamma(u_1, t - \tau) du_1 + \frac{\tau}{\tau_s}. \tag{22}$$

When the electronic relaxation effect is expressed by eq.(14), $\Gamma(\tau)$ becomes

$$\Gamma(\tau) = \frac{\tau_b}{\tau_a} \left(\frac{\tau}{\tau_b} + e^{-\frac{\tau}{\tau_b}} - 1 \right) + \frac{\tau}{\tau_s}. \tag{23}$$

The electric polarization P is given as

$$\begin{aligned}
P &= N_t \text{Tr}(\rho R) = N_t \sum_{c,v} (\rho_{cv} R_{vc} + \rho_{vc} R_{cv}) \\
&= j \frac{N_t}{\hbar} \sum_c \sum_v (\rho_{vv} - \rho_{cc}) |R_{cv}|^2
\end{aligned}$$

$$\{\Phi(\omega)E_\omega e^{j\omega t} - \Phi(\omega)^* E_\omega^* e^{-j\omega t}\}, \quad (24)$$

where N_t is the density of electrons including both the conduction and the valence bands. The susceptibility $\chi(\omega)$ is defined by the relation of

$$P = \varepsilon_0 \{\chi(\omega)E_\omega e^{j\omega t} + \chi^*(\omega)E_\omega^* e^{-j\omega t}\}, \quad (25)$$

and is written as

$$\chi(\omega) = j \frac{N_t}{\varepsilon_0 \hbar} \sum_c \sum_v (\rho_{vv} - \rho_{cc}) |R_{cv}|^2 \Phi(\omega). \quad (26)$$

Then the absorption coefficient α_{vc} due to the interband transition is written as

$$\begin{aligned} \alpha_{vc} &= \frac{\sqrt{\mu_0 \varepsilon_0}}{n_r} \omega \text{Im}\{\chi(\omega)\} \\ &= \sqrt{\frac{\mu_0}{\varepsilon_0}} \frac{\omega}{n_r} N_t \sum_c \sum_v (\rho_{vv} - \rho_{cc}) |R_{cv}|^2 S(\hbar\omega - W_{cv}), \end{aligned} \quad (27)$$

where n_r is the refractive index and $S(\hbar\omega - W_{cv})$ is the spectral line shape function given in this section as

$$\begin{aligned} S(\hbar\omega - W_{cv}) &\equiv \frac{1}{\hbar} \text{Re}\{\Phi(\omega)\} \\ &= \frac{1}{\hbar} \text{Re} \left\{ \int_0^\infty \exp\{j(\omega_{cv} - \omega)\tau - \overline{\Gamma(\tau)}\} d\tau \right\}. \end{aligned} \quad (28)$$

A specific feature of this paper is the introduction of this spectral line shape function. The spectral line shape function explains well the absorption tail extending into the band gap.

3. Franz-Keldysh Effect

3.1 Relationship between dipole moment and electron wave function

The Franz-Keldysh effect is taken into account to modify the value of the dipole moment $|R_{cv}|^2$ in eq.(27). Analysis of the Franz-Keldysh effect in this work is based

on an already established method.¹⁸⁾ A model of the analysis is illustrated in Fig.1. An electron in the conduction or the valence band is defined in a rectangular box whose lengths are L_x , L_y , and L_z . When a DC electric field F is applied along the z-direction, the value of the dipole moment R_{cv} is changed through the change of electron states $|c\rangle$ and $|v\rangle$. A wave function of a single electron in the j-th band $\Psi_j(\mathbf{r})$ is given with envelope functions $X_j(x)$, $Y_j(y)$, and $Z_j(z)$, which vary moderately, and a periodic function $u_{j\mathbf{k}}(\mathbf{r})$ whose variation is repeated by shifting with the crystal lattice,

Fig.1

$$\Psi_j(\mathbf{r}) = \frac{1}{\sqrt{L_x L_y L_z}} X_j(x) Y_j(y) Z_j(z) u_{j\mathbf{k}}(\mathbf{r}). \quad (29)$$

The subscript j stands for the conduction band when $j = c$ and the valence band when $j = v$. Matrix element R_{cv} of the dipole moment is written as

$$|R_{cv}|^2 = |\langle \psi_c(\mathbf{r}) | e\mathbf{r} | \psi_v(\mathbf{r}) \rangle|^2 \simeq |R_0|^2 |I_x|^2 |I_y|^2 |I_z|^2, \quad (30)$$

where I_x is

$$I_x = \int_{-\frac{L_x}{2}}^{\frac{L_x}{2}} X_c^*(x) X_v(x) dx. \quad (31)$$

I_y and I_z are similarly defined. R_0 is

$$|R_0|^2 = |\langle u_c(\mathbf{r}) | e\mathbf{r} | u_v(\mathbf{r}) \rangle|^2. \quad (32)$$

The optical absorption is given as the sum of $|R_{cv}|^2$ of the dipole moment for all energy levels, as

$$\begin{aligned} & \sum_c \sum_v |R_{cv}|^2 \\ &= \sum_{n_{cx}} \sum_{n_{cy}} \sum_{n_{cz}} \sum_{n_{vx}} \sum_{n_{vy}} \sum_{n_{vz}} |R_0|^2 |I_x|^2 |I_y|^2 |I_z|^2. \end{aligned} \quad (33)$$

where n_{ji} denotes the n-th state of an electron along the i-direction (i=x, y, z) in the j-th band.

3.2 Wave function and number of electron states parallel to applied field

The envelope function $Z_j(z)$ for the z -direction parallel to the applied field F is given by the following Schrödinger equation under the effective-mass approximation.¹⁸⁾

$$\left\{ -\frac{\hbar^2}{2m_j} \frac{\partial^2}{\partial z^2} \pm eFz \right\} Z_j(z) = W_{jz} Z_j(z) \quad (34)$$

Here, m_j is the effective mass of an electron in the j -th band and W_{jz} is the eigenenergy for the z -direction. The $+$ and $-$ signs in eq.(34) refer to an electron in the conduction band and a hole in the valence band, respectively. In the case of a bulk crystal, we set the position of the boundary, $z = \pm L_z/2$, to be $\pm\infty$ with the convergent condition of

$$Z_j\left(\pm\frac{L_z}{2}\right) \rightarrow Z_j(\pm\infty) = 0. \quad (35)$$

By transforming the variable z in eq.(34) to ξ_j defined as

$$\xi_j \equiv \left(\frac{2m_j eF}{\hbar^2}\right)^{\frac{1}{3}} \left[-\frac{W_{jz}}{eF} \pm z\right], \quad (36)$$

eq.(34) is rewritten as

$$\left\{ \frac{\partial^2}{\partial \xi_j^2} - \xi_j \right\} Z_j(\xi_j) = 0. \quad (37)$$

Using one of the boundary conditions in eq.(35), $Z_c(\infty) = 0$ or $Z_v(-\infty) = 0$, the solution to eq.(37) becomes¹²⁾

$$Z_j(z) = a_j Ai(\xi_j), \quad (38)$$

where $Ai(\xi)$ is the Airy function defined by

$$Ai(\xi) = \frac{1}{\pi} \int_0^\infty \cos\left(\frac{u^3}{3} + \xi u\right) du \quad (39)$$

and a_j is a normalization constant given by

$$a_j \simeq \sqrt{\pi} \left(\frac{2}{L_z} \right)^{\frac{1}{4}} \left(\frac{2m_j eF}{\hbar^2} \right)^{\frac{1}{12}}. \quad (40)$$

Then the envelope integration I_z becomes, for $L \rightarrow \infty$,

$$I_z \simeq \pi \sqrt{\frac{2}{L_z}} \left[\frac{(\hbar M_{vc})^2}{2eF} \right]^{\frac{1}{6}} \frac{1}{(m_c m_v)^{\frac{1}{4}}} \text{Ai} \left[- \left\{ \frac{2M_{vc}}{(\hbar eF)^2} \right\}^{\frac{1}{3}} (W_{cz} + W_{vz}) \right]. \quad (41)$$

By applying the other boundary condition of $Z_c(-\infty) \rightarrow 0$ or $Z_v(\infty) \rightarrow 0$ to eq.(38), we obtain

$$\sin \left[\frac{2}{3} \left(\frac{2m_j eF}{\hbar^2} \right)^{\frac{1}{2}} \left(\frac{W_{jz}}{eF} + \frac{L_z}{2} \right)^{\frac{3}{2}} + \frac{\pi}{4} \right] \simeq 0. \quad (42)$$

Therefore the eigenenergy W_{jz} can be determined by

$$n_{jz} = \frac{2}{3\pi} \left(\frac{2m_j eF}{\hbar^2} \right)^{\frac{1}{2}} \left(\frac{W_{jz}}{eF} + \frac{L_z}{2} \right)^{\frac{3}{2}} + \frac{1}{4} \\ (n_{jz} = 1, 2, 3, \dots). \quad (43)$$

The density of states per unit energy for the z-direction under the limit of $L_z \rightarrow \infty$ is given, with the help of eq.(43), as

$$\frac{dn_{jz}}{dW_{jz}} = \frac{1}{\pi} \left(\frac{2m_j eF}{\hbar^2} \right)^{\frac{1}{2}} \left(\frac{W_{jz}}{eF} + \frac{L_z}{2} \right)^{\frac{1}{2}} \frac{1}{eF} \\ \simeq \frac{1}{\pi \hbar} \left(\frac{m_j L_z}{eF} \right)^{\frac{1}{2}}. \quad (44)$$

The summation over n_{cz} and n_{vz} is replaced by the integral $\int \int dW_{cz} dW_{vz}$.

$$\sum_{n_{cz}} \sum_{n_{vz}} \\ = \int_{-\frac{eFL_z}{2}}^{\infty} \int_{-\frac{eFL_z}{2}}^{\infty} \frac{dn_{cz}}{dW_{cz}} \frac{dn_{vz}}{dW_{vz}} dW_{cz} dW_{vz} \\ = \left(\frac{1}{\pi \hbar} \right)^2 \frac{L_z}{eF} (m_c m_v)^{\frac{1}{2}} \int_{-\frac{eFL_z}{2}}^{\infty} \int_{-\frac{eFL_z}{2}}^{\infty} dW_{cz} dW_{vz} \quad (45)$$

Then, we obtain

$$\begin{aligned}
\sum_{n_{cz}} \sum_{n_{vz}} |I_z|^2 &= \frac{1}{W_f^2} \times \\
&\int_{-\frac{eFL_z}{2}}^{\infty} \int_{-\frac{eFL_z}{2}}^{\infty} \left| \text{Ai} \left(-\frac{W_{cz} + W_{vz}}{W_f} \right) \right|^2 dW_{cz} dW_{vz} \\
&\simeq \frac{eFL_z}{W_f^2} \int_{-eFL_z}^{\infty} \left| \text{Ai} \left(-\frac{W_z}{W_f} \right) \right|^2 dW_z,
\end{aligned} \tag{46}$$

where W_f is defined as $W_f = \{(\hbar eF)^2/2M_{vc}\}^{1/3}$ with reduced mass of M_{vc} defined as $1/M_{vc} = 1/m_c + 1/m_v$, and W_z is the energy value which is the sum of those in the conduction and valence bands, $W_z = W_{cz} + W_{vz}$.

3.3 Optical absorption coefficient under uniform electric field

Since we are treating an intrinsic semiconductor here, we can set $\rho_{cc} \approx 0$ and $\rho_{vv} \approx 0$, which are electron distribution probabilities in the conduction and valence bands, respectively. The optical absorption coefficient α_{vc} in eq.(27) can be rewritten, using eq.(33), as

$$\begin{aligned}
\alpha_{vc} &= \sqrt{\frac{\mu_0}{\varepsilon_0}} \frac{\omega}{n_r} \frac{2}{L_x L_y L_z} \sum_{n_{cx}} \sum_{n_{cy}} \sum_{n_{cz}} \sum_{n_{vx}} \sum_{n_{vy}} \sum_{n_{vz}} \\
&|R_0|^2 |I_x|^2 |I_y|^2 |I_z|^2 S(\hbar\omega - W).
\end{aligned} \tag{47}$$

The summation of states for the z-direction in eq.(47) is given by eq.(46). Other summations of states within the x-y plane are given by eq.(A·8) in the Appendix. The optical absorption coefficient $\alpha_{vc}(F, \omega)$ under electric field F is

$$\begin{aligned}
&\alpha_{vc}(F, \omega) \\
&= \frac{\omega}{n_r} \sqrt{\frac{\mu_0}{\varepsilon_0}} \frac{M_{vc}}{\pi \hbar^2} \frac{eF}{W_f^2} \\
&\int_0^{\infty} \int_{-eFL_z}^{\infty} |R_0|^2 \left| \text{Ai} \left(-\frac{W_z}{W_f} \right) \right|^2 S(\hbar\omega - W) dW_z dW_{||} \\
&= \frac{\omega}{n_r} \sqrt{\frac{\mu_0}{\varepsilon_0}} \frac{M_{vc}}{\pi \hbar^2} \frac{eF}{W_f^2}
\end{aligned}$$

$$\int_{-\infty}^{\infty} |R_0|^2 \left\{ \frac{W - W_g}{W_f} \left| Ai \left(-\frac{W - W_g}{W_f} \right) \right|^2 + \left| Ai' \left(-\frac{W - W_g}{W_f} \right) \right|^2 \right\} S(\hbar\omega - W) dW, \quad (48)$$

where $W = W_z + W_{\parallel} + W_g$, and $Ai'(\xi) (= dAi(\xi)/d\xi)$ is a derivative of the Airy function. Equation (48) is almost the same as that for the Franz-Keldsh effect in previous analyses in the literature, except for the introduction of the spectral line shape function $S(\hbar\omega - W)$.

Optical absorption is caused by electron transitions from the heavy-hole and the light-hole bands to the conduction band. Therefore, the absorption coefficient $\alpha(F, \omega)$ is given as the sum of the two mechanisms in which the heavy and the light hole are denoted with subscripts $v = h$ and $v = l$, respectively,

$$\alpha(F, \omega) = \alpha_{hc}(F, \omega) + \alpha_{lc}(F, \omega). \quad (49)$$

By denoting the absorption coefficient under no electric field as $\alpha(0, \omega)$, change in the absorption coefficient upon the application of electric field is written as

$$\Delta\alpha(F, \omega) = \alpha(F, \omega) - \alpha(0, \omega). \quad (50)$$

4. Numerical Calculation and Discussion

4.1 Spectral line shape function

The spectral line shape function $S(\hbar\omega - W_{cv})$ was defined in eq.(28) of § 2.2 as a real part of Fourier transformation for time variation of a dipole. Since the analytical solution of eq.(28) is hardly obtained, we must evaluate the equation using suitable approximations and numerical calculations. The integration in the bracket in eq.(28) is written as $I_0(a_1, a_2)$ and defined as

$$I_0(a_1, a_2) = \int_0^{\infty} e^{-a_1 t - a_2 (e^{-\frac{t}{\tau_b}} + \frac{t}{\tau_b} - 1)} dt. \quad (51)$$

$I_0(a_1, a_2)$ can be expanded with a continuing fraction ³⁷⁾

$$I_0(a_1, a_2) = \frac{1}{a_1 + \frac{a_2(1/\tau_b)^2}{a_1 + \frac{1}{\tau_b} + \frac{2a_2(1/\tau_b)^2}{a_1 + 2\frac{1}{\tau_b} + \frac{3a_2(1/\tau_b)^2}{\dots}}}}. \quad (52)$$

Then eq.(28) can be rewritten as

$$S(\hbar\omega - W_{cv}) = \frac{1}{\hbar} Re \left\{ I_0 \left(j \frac{\hbar\omega - W_{cv}}{\hbar} + \frac{1}{\tau_s}, \frac{\tau_b}{\tau_a} \right) \right\}. \quad (53)$$

In the case of $\tau_b/\tau_a \gg 1$, the shape function becomes Gaussian,

$$S(\hbar\omega - W_{cv}) = \sqrt{\pi} \frac{1}{\hbar} \sqrt{\frac{\tau_a \tau_b}{2}} e^{-\left[\frac{\hbar\omega - W_{cv}}{\hbar} \sqrt{\frac{\tau_a \tau_b}{2}} \right]^2}, \quad (54)$$

while in case of $\tau_b/\tau_a \ll 1$, the function is Lorentzian.

$$S(\hbar\omega - W_{cv}) = \frac{\hbar/\tau_a}{(\hbar\omega - W_{cv})^2 + (\hbar/\tau_a)^2} \quad (55)$$

Numerical calculations in following part of this paper are performed using eqs.(51) and (52). Figure 2 shows the shapes of $S(\hbar\omega - W_{cv})$ for four values of τ_b : 0 fs, 10 fs, 40 fs and 100 fs, with a fixed value of $\tau_a = 0.1$ ps. The curve for $\tau_b = 0$ fs corresponds to the Lorentzian and the curve for $\tau_b = 100$ fs is Gaussian-like Fig.2

4.2 Numerical calculation of optical absorption coefficient

4.2.1 No electronic field

When there is no applied field, we obtain the following relation from eq.(27).

$$\begin{aligned} N_t \sum_c \sum_v & \\ &= g_{cv}(W_{cv}) dW_{cv} \\ &= \frac{1}{2\pi^2 \hbar^3} \left(\frac{2m_c m_v}{m_c + m_v} \right)^{\frac{3}{2}} \sqrt{W_{cv} - W_g} dW_{cv} \end{aligned} \quad (56)$$

Then, the optical absorption coefficient $\alpha_{vc}(0, \omega)$ becomes

$$\alpha_{vc}(0, \omega)$$

$$= \frac{\omega}{n_r} \sqrt{\frac{\mu_0}{\varepsilon_0}} \int_{W_g}^{\infty} |R_0|^2 g_{cv}(W_{cv}) S(\hbar\omega - W_{cv}) dW_{cv}. \quad (57)$$

The total optical absorption coefficient $\alpha(0, \omega)$ is given as a sum of $v = h$ and $v = l$, as discussed in eq.(49).

Material parameters of the GaAs crystal used for numerical calculation are $n_r = 3.6$, $m_c = 0.067m_0$, $m_h = 0.45m_0$, $m_l = 0.082m_0$, $W_g = 1.42 \text{ eV}$, and $|R_0|^2 = 5.79 \times 10^{-57} (W_g/W)^2 \text{ C}^2\text{m}^2$. Calculated examples of the optical absorption coefficient are shown in Fig.3, where the solid lines are cases in which the electronic intraband relaxation is taken into account, while the dotted line is for the case without taking account of the relaxation. Experimental data from ref. 23 are plotted with the black circles. The absorption tail observed in experiment is explained well by the electronic relaxation effect with the parameters of $\tau_a = 0.1 \text{ ps}$, $\tau_b = 40 \text{ fs}$ and $\tau_s = 1 \text{ ns}$, in this example.

Fig.3

4.2.2 Optical absorption coefficient under applied DC electric field

The calculated optical absorption coefficient in an intrinsic GaAs crystal under applied DC electric field is shown in Fig.4 with experimental data obtained by Casey *et al.*²³⁾ and Stillman *et al.*¹⁾ The solid and the dotted lines in Fig.4 are calculated data with and without taking account of the electric intraband relaxation, respectively. The absorption in the band gap becomes stronger with stronger applied field. The experimental data are explained well by our theoretical calculation where the electronic intraband relaxation effect is taken into account. Calculated data of the change $\Delta\alpha(F, \omega)$ in the absorption coefficient are shown in Figs.5 and 6, where the solid lines and dotted lines are for with and without taking account of the intraband relaxation effect, respectively. The energy distribution of $\Delta\alpha(F, \omega)$ is smoothed by taking into account the relaxation effect, as shown in Fig.5.

Fig.4

Fig.5

Fig.6

4.3 Change in refractive index due to applied electric field

Real and imaginary parts of the dielectric constant are generally combined with the Kramers-Krönig relation. Denoting the change in the refractive index induced by applying electric field as $\Delta n(F, \omega)$, $\Delta n(F, \omega)$ is derived from $\Delta\alpha(F, \omega)$ as

$$\Delta n(F, \omega) = \frac{c}{\pi} \int_0^\infty \frac{\Delta\alpha(F, \omega')}{\omega'^2 - \omega^2} d\omega', \quad (58)$$

where c is the speed of light. Change in the refractive index Δn is numerically calculated, as shown in Figs.7 and 8, from data in Figs.5 and 6. The black circles in Fig.7 indicate experimental data obtained by Pond *et al.*²⁰⁾ Our theoretical calculations coincide well with the experimental data.

Fig.7

Fig.8

5. Conclusions

The optical absorption coefficient and the refractive index due to the Franz-Keldysh effect were theoretically analyzed by taking into account the electronic intraband relaxation phenomena.

- A treatment basing on the density matrix formalism with a stochastic model was performed to take into account the electronic relaxation phenomena in a more exact form.
- The absorption tail observed in experiment is explained to be a result of the electronic intraband relaxation.
- The experimental data on the Franz-Keldsh effect were explained well using our improved theory.

References

- 1) G. E. Stillman, C. M. Wolfe, C.O. Bozler and J.A. Rossi: Appl. Phys. Lett. **28** (1976) 544.
- 2) N. K. Dutta and N. A. Olsson: Electron. Lett. **20** (1984) 634.
- 3) Y. Noda, M. Suzuki, Y. Kushiro and S. Akiba: J. Lightwave Technol. **4** (1986) 1445.
- 4) T. E. Van Eck, L. M. Waipita, W. S. C. Chang and H. H. Wieder: Appl. Phys. Lett. **48** (1986) 451.
- 5) A. Alping and L. A. Coldren: J. Appl. Phys. **61** (1987) 2430.
- 6) H. Soda, K. Nakai, H. Ishikawa and H. Imai: Electron. Lett. **23** (1987) 1232.
- 7) J. G. Mendoza, L. A. Coldren, A. Alping, R. H. Yan, T. Hausken, K. Lee and K. Pedrotti: IEEE J. Lightwave Technol. **6** (1988) 793.
- 8) B. R. Bennett and R. A. Soref: IEEE J. Quantum Electron. **23** (1987) 2159.
- 9) G. Mak, C. Rolland, K. E. Fox and C. Blaauw: IEEE Photon. Tech. Lett. **2** (1990) 730.
- 10) W. Franz: Z. Naturforsch. **Teil A 13** (1958) 484.
- 11) L. V. Keldysh: Sov. Phys. JETP **34** (1958) 788.
- 12) K. Tharmalingam: Phys. Rev. **130** (1963) 2204.
- 13) J. Callaway: Phys. Rev. **134** (1964) A998.
- 14) B. O. Seraphin and N. Bottka: Phys. Rev. **139** (1965) A560.
- 15) B. O. Seraphin and N. Bottka: Phys. Rev. **145** (1966) 628.
- 16) D. E. Aspnes: Phys. Rev. **147** (1966) 554.
- 17) D. E. Aspnes: Phys. Rev. **153** (1967) 153.
- 18) D. A. B. Miller, D. S. Chemla and S. Schmitt-Rink: Phys. Rev. B **33** (1986) 6976.
- 19) E. G. S. Painge and H. D. Rees: Phys. Rev. Lett. **16** (1966) 444.
- 20) S. F. Pond and P. Handler: Phys. Rev. B **6** (1972) 2248.
- 21) S. F. Pond and P. Handler: Phys. Rev. B **8** (1973) 2869.
- 22) D. E. Aspnes and A. A. Studna: Phys. Rev. B **7** (1973) 4605.

- 23) H. C. Casey, Jr., D. D. Sell and K. W. Wecht: J. Appl. Phys. **46** (1975) 250.
- 24) E. O. Kane: Phys. Rev. **131** (1963) 79.
- 25) B. I. Halperin and M. Lax: Phys. Rev. **148** (1966) 722.
- 26) G. Lasher and F. Stern: Phys. Rev. **133** (1964) A553.
- 27) H. C. Casey, Jr. and F. Stern: J. Appl. Phys. **47** (1976) 631.
- 28) M. Yamada and Y. Suematsu: J. Appl. Phys. **52** (1981) 2653.
- 29) M. Yamada and H. Ishiguro: Jpn. J. Appl. Phys. **20** (1981) 1279.
- 30) M. Yamanishi: Tech. Rep. Opt. Quantum Electron., IEICE, Japan, OQE80-103 (1981) 19 [in Japanese].
- 31) M. Yamanishi and Y. Lee: IEEE J. Quantum Electron. **23** (1987) 367.
- 32) M. Asada: IEEE J. Quantum Electron. **25** (1989) 2019.
- 33) T. Ohtoshi and M. Yamanishi: IEEE J. Quantum Electron. **27** (1991) 46.
- 34) M. Takeshima: Phys. Rev. B **36** (1987) 8082.
- 35) N. Bloembergen: *Nonlinear Optics* (Benjamin, New York, 1965) p. 20.
- 36) A. Tomita and A. Suzuki: IEEE J. Quantum Electron. **27** (1991) 1630.
- 37) T. Takagahara, E. Hanamura and R. Kubo: J. Phys. Soc. Jpn. **43** (1977) 811.
- 38) E. Hanamura: J. Phys. Soc. Jpn. **52** (1983) 2258.

Appendix: Number of Electron States in a x-y Plane Perpendicular to the Applied Field

The envelope functions $X_j(x)$ and $Y_j(y)$ perpendicular to the applied electric field are respectively written as

$$X_j(x) = \sqrt{\frac{2}{L_x}} \sin \left[k_{jx} \left(x + \frac{L_x}{2} \right) \right] \quad (\text{A}\cdot\text{1})$$

$$Y_j(y) = \sqrt{\frac{2}{L_y}} \sin \left[k_{jy} \left(y + \frac{L_y}{2} \right) \right], \quad (\text{A}\cdot\text{2})$$

with the boundary conditions

$$X_j \left(\pm \frac{L_x}{2} \right) = Y_j \left(\pm \frac{L_y}{2} \right) = 0, \quad (\text{A}\cdot\text{3})$$

where k_{jx} and k_{jy} are the wave vector of an electron for x- and y-directions, respectively. Applying the boundary conditions of eq.(A-3) give the following conditions for the state of an electron:

$$k_{jx}L_x = n_{jx}\pi \quad (n_{jx} = 1, 2, 3, \dots) \quad (\text{A}\cdot\text{4})$$

$$k_{jy}L_y = n_{jy}\pi \quad (n_{jy} = 1, 2, 3, \dots), \quad (\text{A}\cdot\text{5})$$

where n_{jx} and n_{jy} denote the n-th state of an electron along x- and y-directions, respectively. Substituting eqs.(A-1) and (A-2) into eq.(31), we get the following equations for the conditions of $L_x = L_y \rightarrow \infty$.

$$\begin{aligned} |I_x|^2 &= \frac{1}{L_x^2} \frac{\sin^2\{(k_{cx} - k_{vx})L_x\}}{(k_{cx} - k_{vx})^2} \\ &\simeq \frac{\pi}{L_x} \delta(k_{cx} - k_{vx}) \end{aligned} \quad (\text{A}\cdot\text{6})$$

$$\begin{aligned}
|I_y|^2 &= \frac{1}{L_y^2} \frac{\sin^2\{(k_{cy} - k_{vy})L_y\}}{(k_{cy} - k_{vy})^2} \\
&\simeq \frac{\pi}{L_y} \delta(k_{cy} - k_{vy})
\end{aligned} \tag{A.7}$$

The sum of all states of eq.(33), $\sum_{n_{cx}} \sum_{n_{cy}} \sum_{n_{vx}} \sum_{n_{vy}} |I_x|^2 |I_y|^2$, is given, using eqs.(A.6) and (A.7), as

$$\begin{aligned}
&\sum_{n_{cx}} \sum_{n_{cy}} \sum_{n_{vx}} \sum_{n_{vy}} |I_x|^2 |I_y|^2 \\
&= \left(\frac{L_x}{\pi}\right) \left(\frac{L_y}{\pi}\right) \int \int \int \int \\
&\quad \delta(k_{cx} - k_{vx}) \delta(k_{cy} - k_{vy}) dk_{cx} dk_{cy} dk_{vx} dk_{vy} \\
&= \frac{L_x L_y}{2\pi} \int_0^{k_{\parallel}} k_{\parallel} dk_{\parallel} = \frac{L_x L_y M_{vc}}{2\pi \hbar^2} \int dW_{\parallel},
\end{aligned} \tag{A.8}$$

where

$$k_{\parallel}^2 = k_{cx}^2 + k_{cy}^2 \tag{A.9}$$

$$W_{\parallel} = \frac{\hbar^2}{2m_c} (k_{cx}^2 + k_{cy}^2) + \frac{\hbar^2}{2m_v} (k_{vx}^2 + k_{vy}^2) \tag{A.10}$$

and

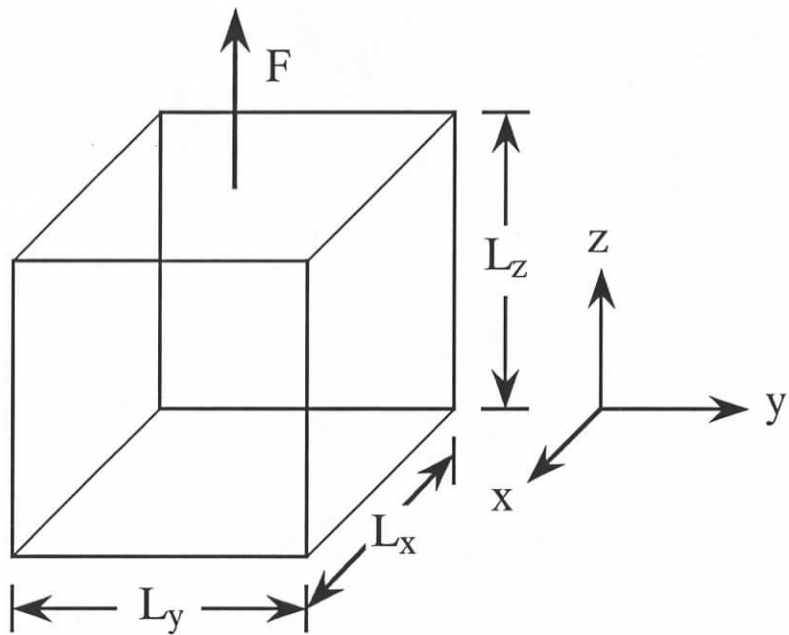
$$\frac{1}{M_{vc}} = \frac{1}{m_c} + \frac{1}{m_v} \tag{A.11}$$

are used.

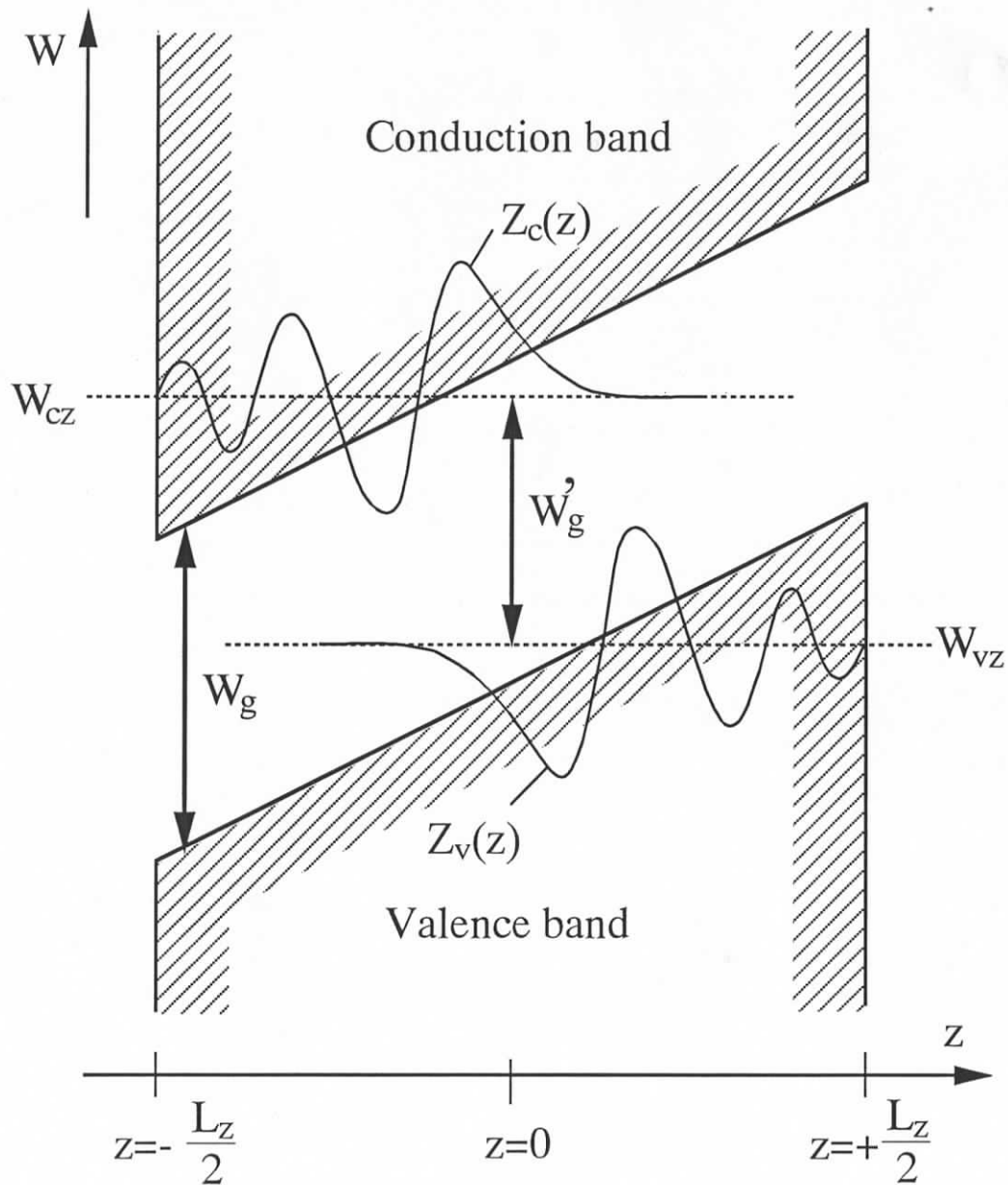
Figure captions

- Fig. 1. Analytical model of Franz-Keldysh effect. (a) An electron is confined in a semiconductor with a rectangular box with lengths of L_x , L_y , and L_z and a DC electric field F applied along the z -direction. (b) Envelope functions of electron wave, $Z_v(z)$ and $Z_c(z)$, in the valence and the conduction bands for the z -direction parallel to the applied field.
- Fig. 2. Spectral line shape function $S(\hbar\omega - E)$ for several correlation time values. The values of the parameters are $\tau_s=1$ ns, $\tau_a=0.1$ ps.
- Fig. 3. Optical absorption coefficient under no electronic field for undoped GaAs. The solid lines are examples calculated for several correlation time values, taking into account the electronic intraband relaxation, and the dotted line is the case of not taking into account the relaxation. Black circles are experimental data reported by Casey *et al.* in ref. 23.
- Fig. 4. Optical absorption coefficient under applied DC electric field for undoped GaAs. The solid and dotted lines are calculated with and without taking into account the electric intraband relaxation, respectively. The values of the parameters for the solid lines are $\tau_a = 0.1$ ps, $\tau_b = 40$ fs, and $\tau_s = 1$ ns. The experimental data are from refs. 1 and 23.
- Fig. 5. Spectrum of change in the absorption coefficient induced by applying electric field. The solid and dotted lines are calculated with and without taking into account the electric intraband relaxation, respectively.
- Fig. 6. Applied electric field dependence of change in the absorption coefficient at fixed photon energies. The solid and dotted lines are calculated with and without taking into account the electric intraband relaxation, respectively.
- Fig. 7. Change in the refractive index induced by applied electric field. The solid and dotted lines are calculated from data in Fig. 5 using eq.(58). The black circles show experimental data under an applied electric field of $F = 7 \pm 1 \times 10^4$ v/cm measured by Pond and Handler.²⁰⁾
- Fig. 8. Applied electric field dependence of the change in refractive index at various photon energies.

Fig. 1 Y. Kawamura et al.



(a)



(b)

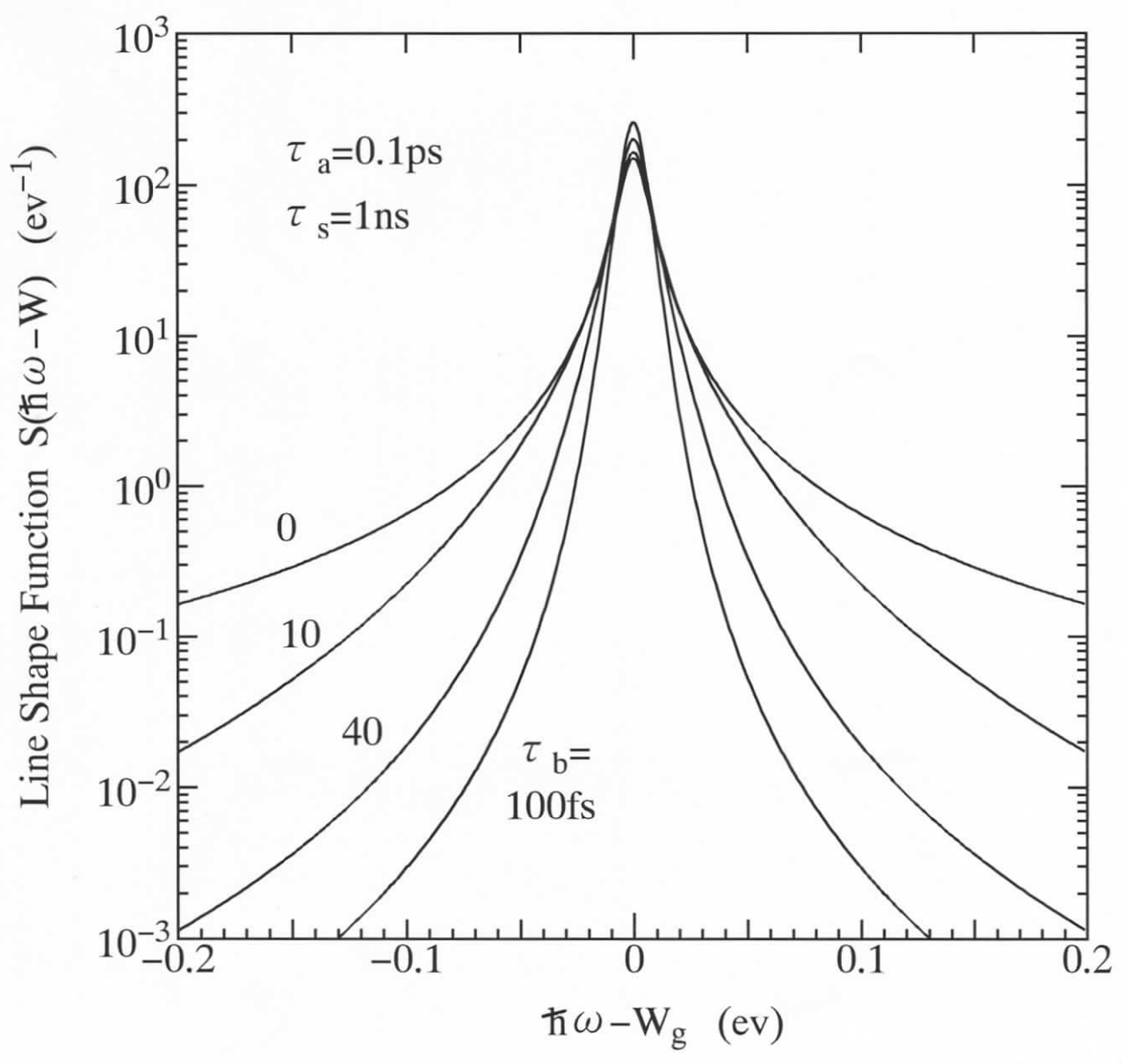


Fig. 2 Y. Kuwamura et al.

"Analysis of Modified Franz-Keldysh ..."

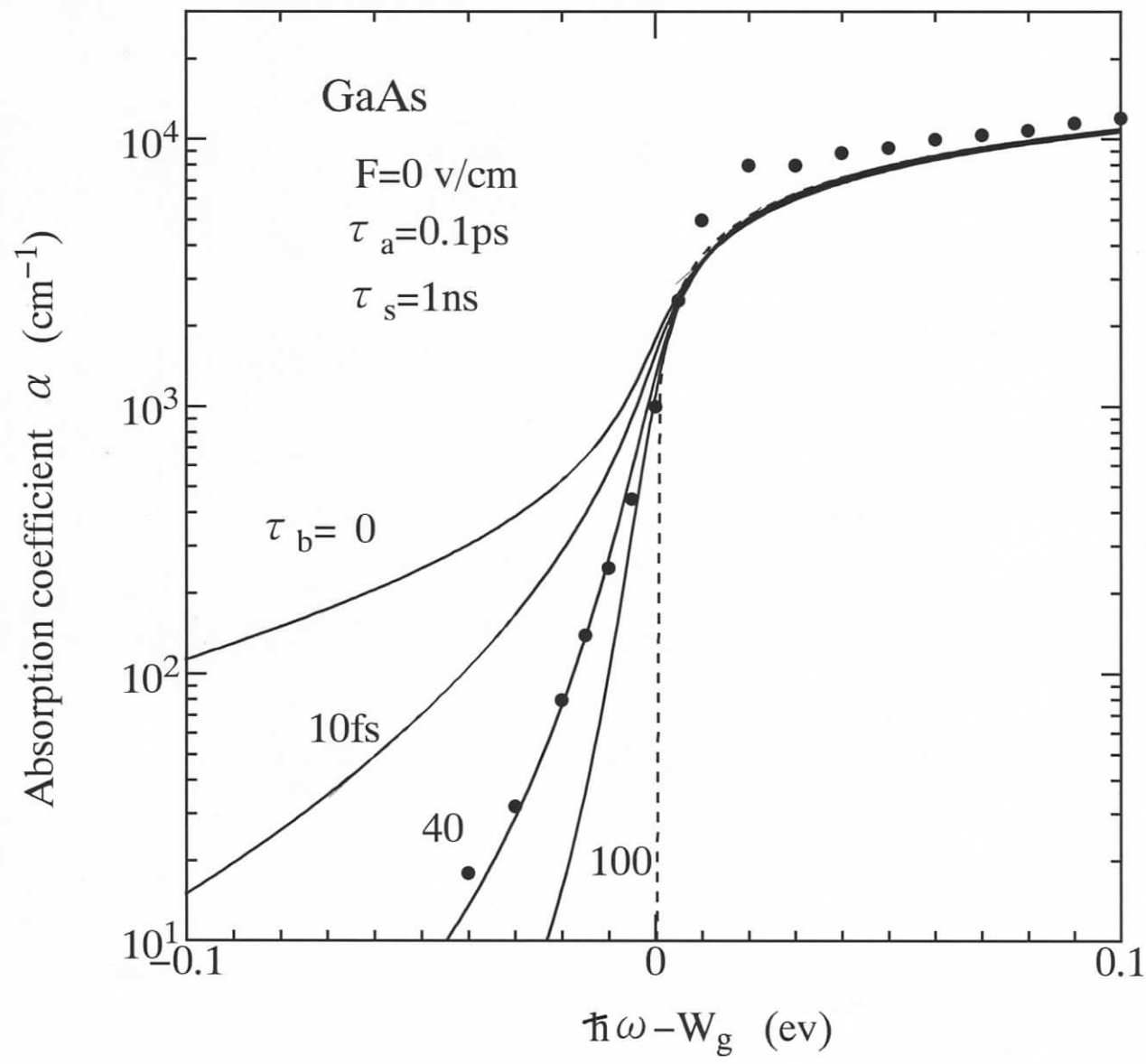


Fig. 3 Y. Kuwamura et. al.

"Analysis of Modified Franz-Keldysh - - -"

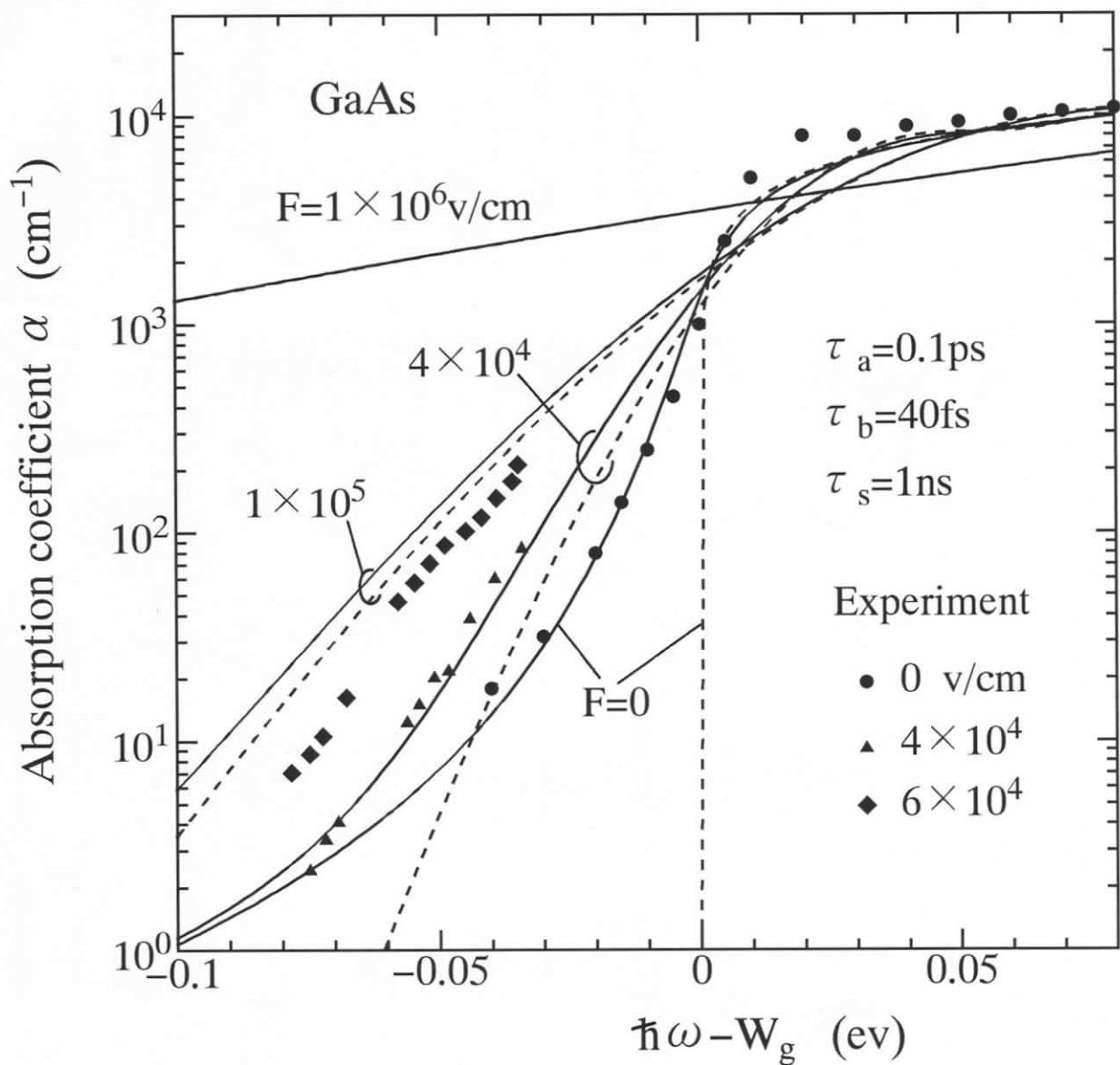


Fig. 4 Y. Kuwamura et. al.

"Analysis of Modified Franz-Keldysh"

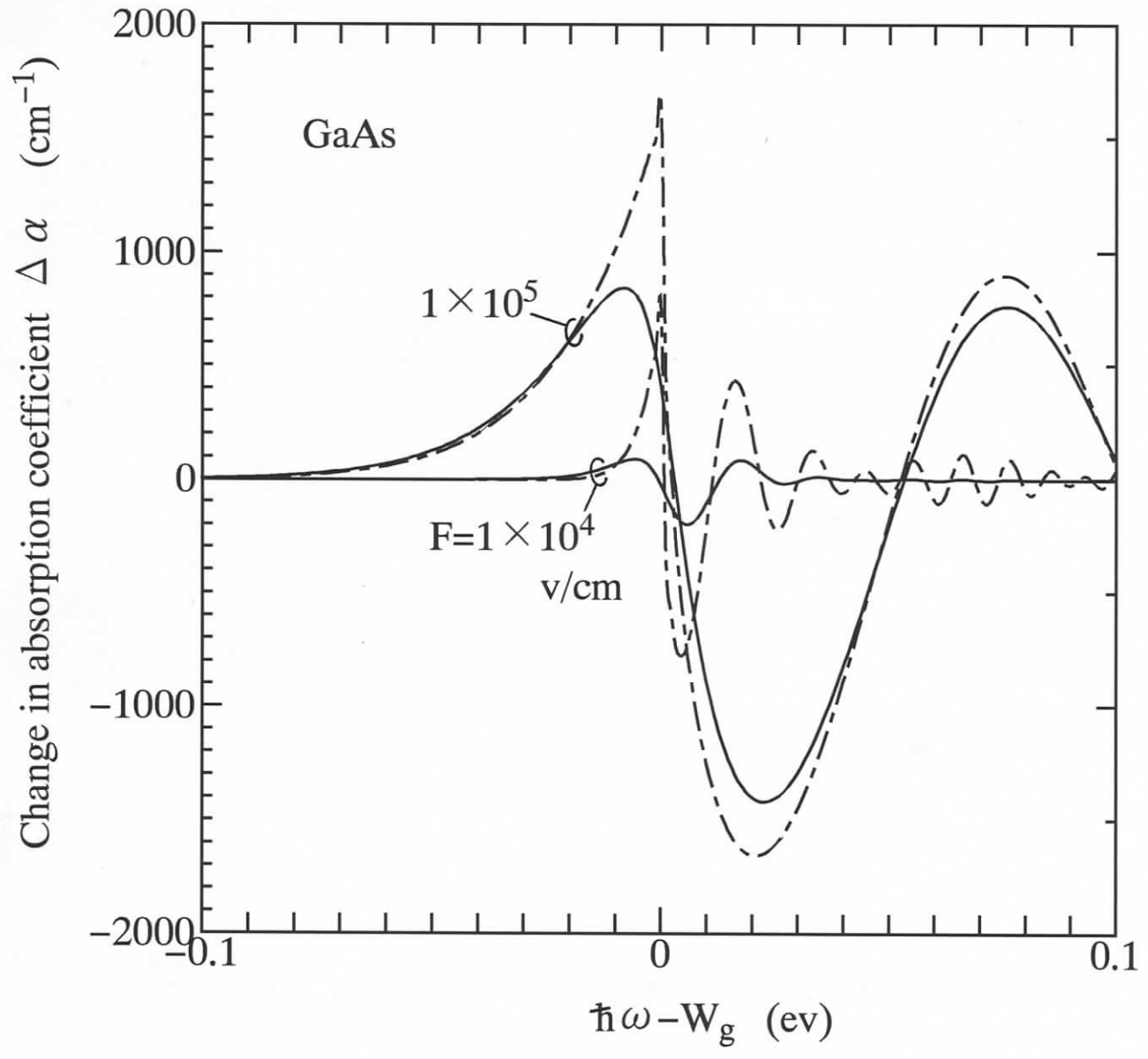


Fig. 5 Y. Kuwamura et al.

"Analysis of Modified Franz-Keldysh

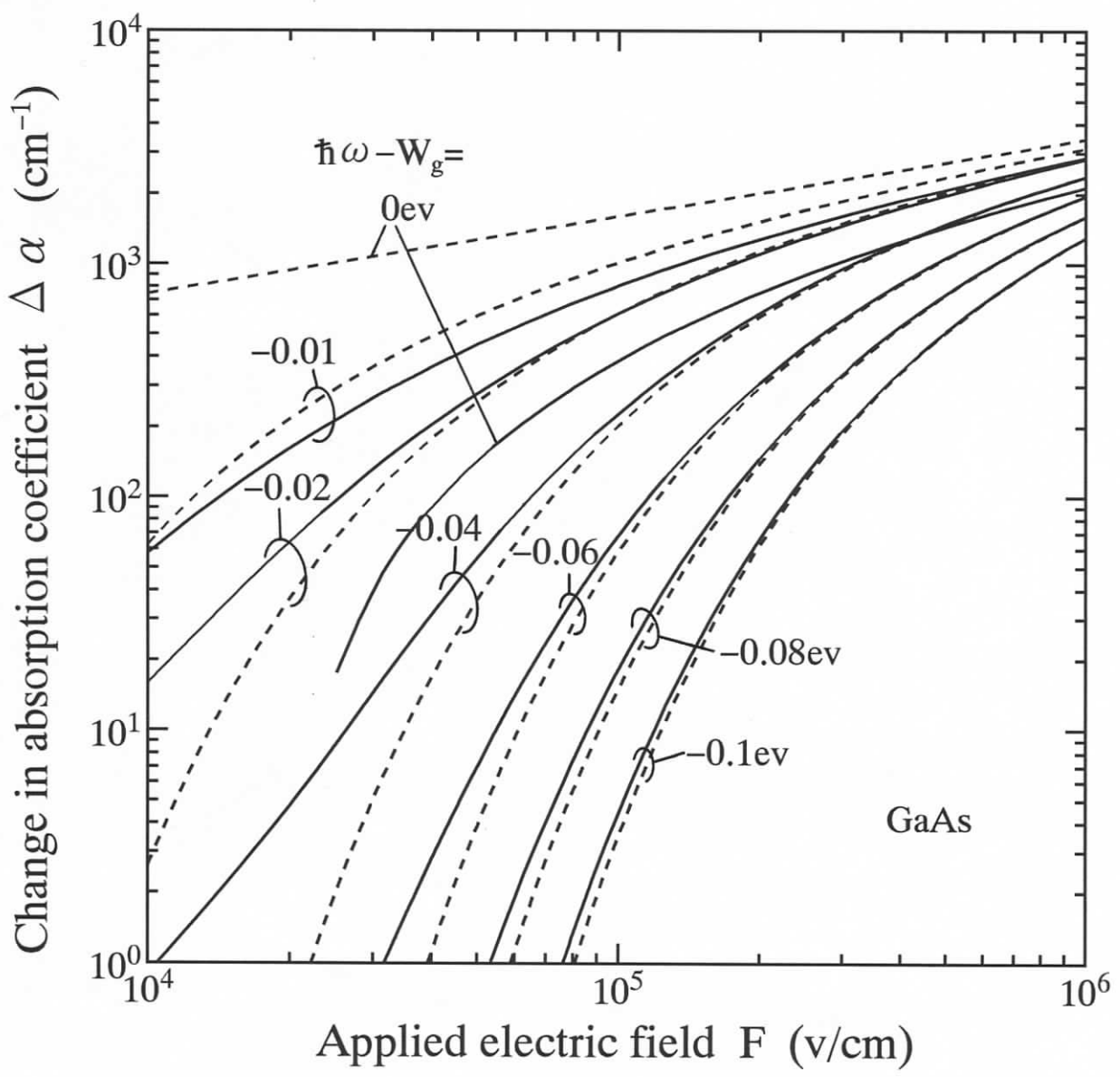


Fig. 6 Y. Kuwamura et al.

"Analysis of Modified Franz-Keldysh - - - -"

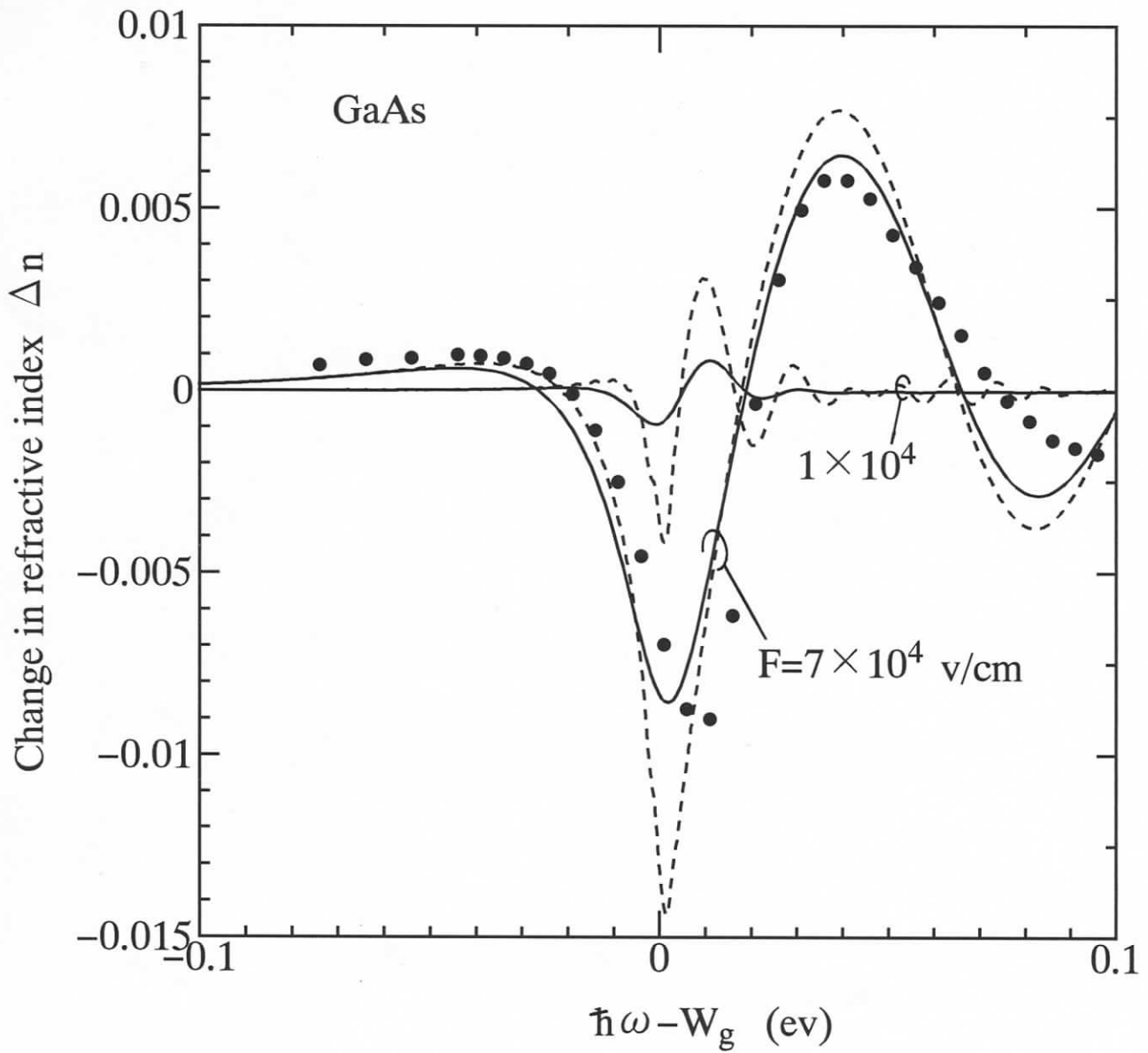


Fig. 7 Y. Kuwamura et al.

"Analysis of Modified Franz-Keldysh ---"

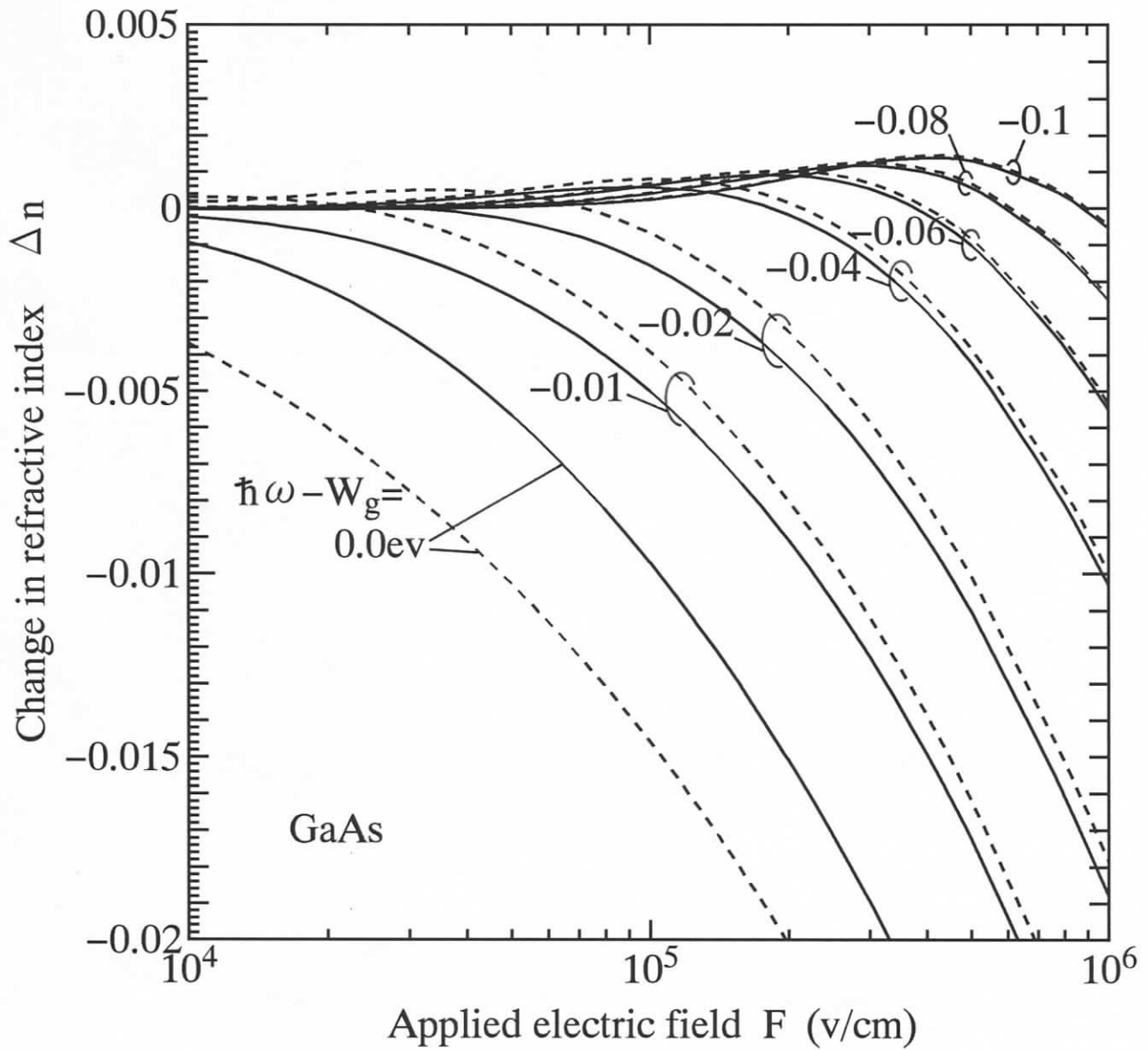


Fig. 8 Y. Kuwamura et al.

"Analysis of Modified Franz-Keldysh - - - -"